

BROADBAND PREDICTION OF WIND-INDUCED DISTURBANCES

A. Hoffmann, R. Luckner†*

Technische Universität Berlin,
Institut für Luft- und Raumfahrt
Flugmechanik, Flugregelung und Aeroelastizität
Marchstraße 12, Berlin, Germany

Abstract

For automatic flight control, indicated airspeed V_{IAS} , angle of attack (AOA) and altitude have to be measured. This can be achieved by absolute and differential pressure sensors. As pressure sensor signals are noisy, they have to be filtered. Another influence on the sensor signals is atmospheric turbulence (process noise). An optimal filter solution in presence of measurement and process noise is a continuous Kalman-Bucy filter. The observer structure of the filter allows signal quality improvement and broadband estimation of immeasurable states. The system model that is needed for filter design is the flight mechanical model of the longitudinal aircraft motion combined with Dryden's model of turbulence. With such a model, the two immeasurable states, the wind-induced angle of attack α_w and the wind velocity V_w can be estimated. The estimated states can be used for effective feed-forward gust alleviation up to the frequency range of the short period mode. For proof of this filter concept and its robustness, different kinds of disturbances such as discrete gusts and a bias in the α measurement are simulated and discussed.

NOMENCLATURE

Acronyms

ADS	=	air data system
AOA	=	angle of attack
AOSS	=	angle of sideslip
(E)KF	=	(extended) Kalman filter
UAS	=	unmanned aerial system
UAV	=	unmanned aerial vehicle

Letters and Symbols

α	=	angle of attack
\underline{A}	=	system matrix
\underline{B}	=	input matrix
\underline{C}	=	measurement matrix
\underline{E}	=	disturbance matrix
\underline{F}	=	disturbance correction matrix
γ	=	flight path angle
H	=	altitude
\underline{H}	=	Kalman filter gain matrix
n	=	number of states
η	=	elevator deflection angle
η_F	=	thrust power setting
L	=	characteristic wave length
λ	=	Eigen values of the system
ω	=	characteristic cut off frequency
\underline{P}	=	estimation error covariance matrix
q	=	pitch rate

P	=	probability distribution
θ	=	measurement noise
Θ	=	pitch angle
r	=	white noise source
σ	=	standard deviation
\underline{u}	=	input vector
u	=	velocity component in x direction
w	=	velocity component in z direction
V	=	velocity
\underline{x}	=	state vector
ξ	=	process noise (model uncertainties)
\underline{y}	=	output vector
\underline{z}	=	disturbance vector
$\underline{\Theta}$	=	measurement noise covariance matrix
$\underline{\Xi}$	=	process noise covariance matrix

Index

A	=	aerodynamic
a/c	=	aircraft
b	=	body fixed
Dry	=	Dryden
g	=	geodetic
K	=	trajectory fixed
meas	=	measurement
W	=	wind
0	=	reference state

* Dipl.-Ing. Arndt Hoffmann, research scientist, Berlin Institute of Technology, Department of aerospace engineering, DGLR member

† Prof. Dr.-Ing Robert Luckner, Berlin Institute of Technology, Department of aerospace engineering, DGLR member

1 INTRODUCTION

For automatic flight control, indicated airspeed V_{IAS} , angle of attack (AOA) and altitude have to be measured. This information about the air flow condition can be measured by absolute and differential pressure sensors (Prandtl and 4-hole probe). As pressure sensor signals are noisy they have to be filtered. Another influence on the sensor signals is atmospheric turbulence (process noise). An optimal filter solution for compensation of measurement and process noise is a continuous Kalman-Bucy filter. The Kalman-Bucy filter is optimal for white process and measurement noise. Turbulence does not have the characteristics of white noise, so this constraint of the Kalman-Bucy Filter derivation is not met. Dryden's model for turbulence is a possible description of process noise and the input of Dryden's model for turbulence is white noise. Therefore, it is suited to extend the flight mechanical model of the longitudinal aircraft motion to develop an observer to filter the needed signals and to estimate the wind angle of attack as well as the wind velocity. The estimated states can be used for broadband feed-forward gust alleviation, to smooth the aircraft's flight and to improve the ride quality or measurement conditions for payload sensors like gravimeters in the frequency range of the short period mode.

In Wise [1] an Extended Kalman Filter (EKF) is used to determine the AOA and AOSS based on the nonlinear six degree-of-freedom equations of motion and a detailed aircraft aerodynamic model. The EKF framework uses inertial measurements of Euler angles, body rates, body acceleration and measurement of dynamic pressure. This approach was successfully flight tested in the X-45 program. Heller [2] and Myschik [3] use a complementary filter approach based on linear equations to determine AOA and AOSS to extend the bandwidth of these signals. Hoffmann [4] picked this approach up and discussed it in presence of disturbance. Braga [5] shows a low computational cost method dealing with time varying noise statistical properties using a new approach for an adaptive EKF. The method is validated in flight path reconstruction application, with simultaneous air data calibration for AOA, AOSS and static pressure sensors. Combining a linear model of the short period motion and Dryden's turbulence model for wind induced AOA, Hoffmann [6] has shown a Kalman-Bucy filter approach for precise and broadband AOA determination in presence of atmospheric turbulence and measurement noise. An approach how wind AOA can be computed using relations of flight mechanic variables that can be measured in sufficient quality is shown in Hahn [7].

The following explanations are related to the Unmanned Aerial System (UAS) developed by students at the chair of Flight Mechanics, Flight Control and Aeroelasticity at Berlin Institute of Technology. A detailed overview on the UAS and a description of its air data system is given in [4] and [6].

The paper is structured as follows: in section 2 the Kalman-Bucy filter approach is explained in detail. Section 3 describes the Kalman-Bucy filter design and in section 4 simulation results are presented.

2 FILTER APPROACH

In presence of measurement and process noise the Kalman-Bucy filter (KF) generates optimal estimations of system states \tilde{x} or output variables \tilde{y} , see ref. [10].

The KF can be used to filter noisy measurements or to estimate immeasurable states, Fig. 1.

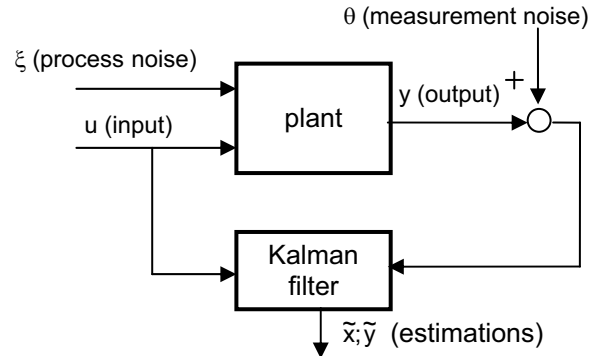


Fig. 1: Kalman filter problem

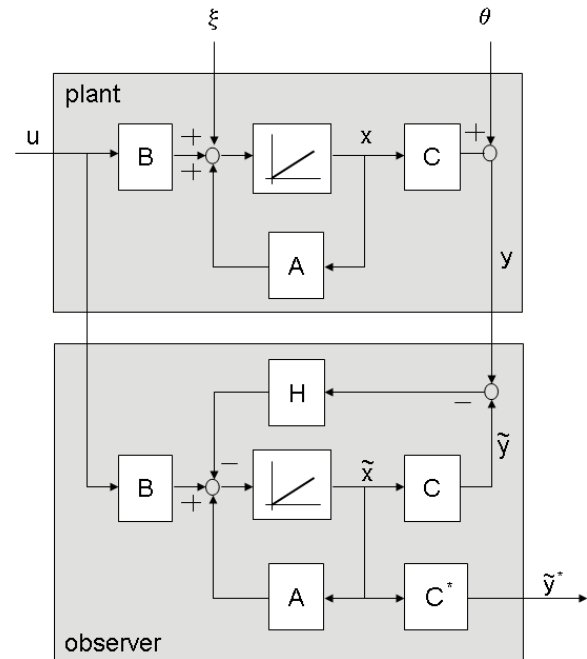


Fig. 2: Plant and Kalman-Bucy

The KF structure is shown in Fig. 2. The system matrix \underline{A} , the input matrix \underline{B} and the measurement matrix \underline{C} describe the linear system dynamics. Estimations are highlighted with \sim such as the state \tilde{x} and output estimations \tilde{y} . Although the base for the filter problem is of a statistical approach, the solution is of the same type as for linear quadratic optimal problems (LQR, Riccati). The KF gain matrix \underline{H} will be calculated in dependency of the process and measurement covariance matrices $\underline{\Xi}$ and $\underline{\Theta}$. For a derivation the reference should be made to [10]. The

optimal KF gain matrix \underline{H} is calculated as follows:

$$\underline{H} = -\underline{\Sigma} \underline{C}^T \underline{\Theta}^{-1} \quad (1)$$

The estimation error covariance matrix $\underline{\Sigma}$ is the positive solution of the quadratic matrix equation, known as Filter Algebraic Riccati Equation (FARE), ref. [10].

$$0 = \underline{A} \underline{\Sigma} + \underline{\Sigma} \underline{A}^T - \underline{\Sigma} \underline{C}^T \underline{\Theta}^{-1} \underline{C} \underline{\Sigma} + \underline{\Xi} \quad (2)$$

The requirements for the existence of an optimal solution are:

- $\underline{\Xi}$ is positive semidefinite, symmetric,
- $\underline{\Theta}$ is positive definite, symmetric,
- the system ($\underline{A}; \underline{C}$) is observable.

These requirements are derived by the assumption of white noise for $\underline{\Theta}$ and $\underline{\Xi}$, ref. [10]. If the optimal state

estimates $\tilde{\underline{x}}$ are computed, the outputs $\tilde{\underline{y}}^*$, including immeasurable states, can be calculated via the additional output matrix \underline{C}^* .

The system model that is necessary for filter design consists of two parts: a linear aircraft model and a disturbance model, in this case Dryden's model for turbulence. These two models are explained in the next two paragraphs and afterwards the coupling to become the system model is described.

Linear state space aircraft model

The dynamics of an aircraft are modeled in a nonlinear form as follows:

$$\begin{aligned} \dot{\underline{x}}_{a/c}(t) &= \underline{a}(\underline{x}_{a/c}(t), \underline{u}_{a/c}(t), \underline{z}(t), t) + \underline{b}(\underline{x}_{a/c}(t), \underline{u}_{a/c}(t)) + \underline{\xi}_1(t) \\ \underline{y}_{a/c}(t) &= \underline{c}(\underline{x}_{a/c}(t), \underline{u}_{a/c}(t), \underline{z}(t), t) + \underline{\theta}(t) \end{aligned} \quad (3)$$

Where $\underline{x}_{a/c}$ is the state vector, $\underline{u}_{a/c}$ is the control input vector, $\underline{\xi}_1$ is the stochastic plant disturbance correlated to model uncertainties, $\underline{y}_{a/c}$ is the measurement vector, $\underline{\theta}$ is the stochastic measurement noise and \underline{z} is the disturbance vector. The functions \underline{a} , \underline{b} and \underline{c} model the nonlinear state dynamics and measurements. The linear aircraft model is derived by Jacobians of this nonlinear 6 degree of freedom model, for horizontal level flight of the aircraft, with respect to the state vector $\underline{x}_{a/c}$, the control input vector $\underline{u}_{a/c}$, the output vector $\underline{y}_{a/c}$ and the disturbance vector \underline{z} . In the resultant linear state space representation for longitudinal motion, the influence of $\underline{x}_{a/c}$, $\underline{u}_{a/c}$, $\underline{y}_{a/c}$, \underline{z} and the noises $\underline{\xi}_1$, $\underline{\theta}$ on the aircraft dynamics and on the measurement can be described as follows:

$$\begin{aligned} \dot{\underline{x}}_{a/c} &= \underline{A}_{a/c} \underline{x}_{a/c} + \underline{B}_{a/c} \underline{u}_{a/c} + \underline{E}_{a/c} \underline{z} + \underline{\xi}_1 \\ \underline{y}_{a/c} &= \underline{C}_{a/c} \underline{x}_{a/c} + \underline{F}_{a/c} \underline{z} + \underline{\theta} \end{aligned} \quad (4)$$

$$\underline{x}_{a/c} = \begin{bmatrix} q_K \\ \alpha_K \\ V_K \\ \Theta \\ H \end{bmatrix}; \quad \underline{u}_{a/c} = \begin{bmatrix} \eta \\ \eta_F \end{bmatrix}; \quad \underline{y}_{a/c} = \begin{bmatrix} q_K \\ \alpha \\ V_A \\ \Theta \\ H \end{bmatrix}; \quad \underline{z} = \begin{bmatrix} \alpha_W \\ V_W \end{bmatrix}$$

The aircraft states are body axis pitch rate q_K , kinematics AOA α_K , flight path velocity V_K , pitch angle Θ and altitude H . The output vector consists of the body axis pitch rate q_K , the AOA α and airspeed V_A as well as the pitch angle Θ and the altitude H . Input is the elevator deflection η as well as the thrust power setting η_F . Wind AOA α_W and wind velocity V_W are the disturbances. For the reference state ($V=20$ m/s; $H=100$ m; $\gamma=0^\circ$; no wind) the numerically derived model is given in the appendix.

Disturbance model

The kinematic relation of aircraft and wind states in the longitudinal motion is shown by the velocity vector equation $\underline{V}_K = \underline{V}_A + \underline{V}_W$ in Figure 3. In this figure x_b is the body fixed reference frame, V_W is the wind speed, V_K is the flight path velocity and V_A is the airspeed. The wind components w_{Wg} , u_{Wg} are defined in the geodetic reference frame (index g). γ is the flight path angle, α is the AOA and α_K is the kinematics AOA. Using the relation shown in Figure 5, the wind AOA α_W can be calculated by equation (5)

$$\sin \alpha_W = \frac{w_{Wg}}{V_A} \cos \gamma - \frac{u_{Wg}}{V_A} \sin \gamma \quad (5)$$

For horizontal flight ($\gamma=0$) and small disturbances the wind AOA α_W follows from the linearized equation

$$\alpha_W = \frac{w_{Wg}}{V_A} \quad (6)$$

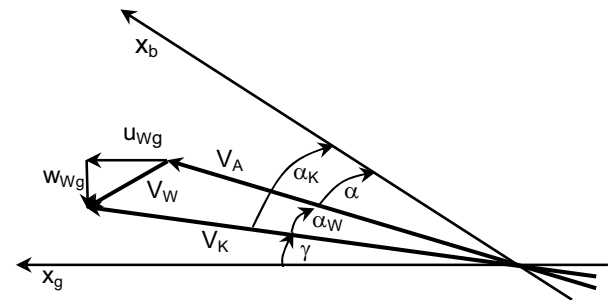


Fig. 3: Velocity vector diagram

Not only the kinematical relations are of interest, a time dependant model for α_W and V_W is needed as well. Dryden's turbulence model is a possible approximation of real gust Power Spectral Density (PSD). To generate these PSD for simulation purpose, white noise $r(t)$ is

sent into a Dryden filter as shown in Fig. 4. For vertical and horizontal turbulence the transfer functions are given by eq. (7) and eq. (8), where σ is the turbulence strength, V_K is the flight path velocity, L is the characteristic wave length, ω is the characteristic cut off frequency and T the characteristic time constant. The index w specifies the vertical wind component and u the horizontal.

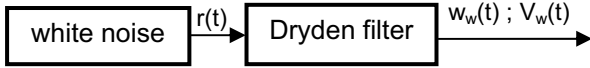


Fig. 4: Turbulence simulation

$$\hat{F}_{ww}(s) = \sqrt{\sigma_w^2 T_w} \frac{1 + s\sqrt{3}T_w}{(1 + sT_w)^2}; \quad T_w = \frac{L_w}{V_K} = \frac{1}{\omega_w} \quad (7)$$

$$\hat{F}_{uw}(s) = \sqrt{2\sigma_u^2 T_u} \frac{1}{(1 + sT_u)}; \quad T_u = \frac{L_u}{V_K} = \frac{1}{\omega_u} \quad (8)$$

The filter characteristics depend on height, atmospheric stability, terrain roughness and wind speed. The characteristic values of the Dryden filter for $V_K=20$ m/s, stable atmosphere, $H=100$ m and medium turbulence $\sigma_u=5$ m/s are, according to [11], as follows:

- $L_w=93$ m, $L_u=100$ m
- $\omega_w=0.2151$ rad/s, $\omega_u=0.2$ rad/s
- $\sigma_w=3.5$ m/s.

Uncertainties in the Dryden filter characteristics are modeled as process noise (ξ_2) in the filter design section. Using the linear equation (6) Dryden's turbulence model can be written in observer state space form as:

$$\begin{aligned} \dot{\mathbf{x}}_{\text{Dry}} &= \mathbf{A}_{\text{Dry}} \mathbf{x}_{\text{Dry}} + \mathbf{B}_{\text{Dry}} \mathbf{r} + \xi_2 \\ \mathbf{z} &= \mathbf{C}_{\text{Dry}} \mathbf{x}_{\text{Dry}} \end{aligned} \quad (9)$$

$$\begin{aligned} \begin{bmatrix} \delta\ddot{\alpha}_w \\ \delta\dot{\alpha}_w \\ \delta\dot{V}_w \end{bmatrix} &= \begin{bmatrix} 0 & -\omega_w^2 & 0 \\ 1 & -2\omega_w & 0 \\ 0 & 0 & -\omega_u \end{bmatrix} \begin{bmatrix} \delta\dot{\alpha}_w \\ \delta\alpha_w \\ \delta V_w \end{bmatrix} + \dots \\ &\dots + \begin{bmatrix} \frac{\sigma_w}{V_0} \sqrt{\omega_w^3} & 0 \\ \frac{\sigma_w}{V_0} \sqrt{3\omega_w} & 0 \\ 0 & \sigma_u \sqrt{2\omega_u} \end{bmatrix} \begin{bmatrix} r_1 \\ r_2 \end{bmatrix} + \begin{bmatrix} \xi_{\dot{\alpha}_w} \\ \xi_{\alpha_w} \\ \xi_{V_w} \end{bmatrix} \\ \begin{bmatrix} \delta\alpha_w \\ \delta V_w \end{bmatrix} &= \begin{bmatrix} 0 & 1 & 0 \\ 0 & 0 & 1 \end{bmatrix} \begin{bmatrix} \delta\dot{\alpha}_w \\ \delta\alpha_w \\ \delta V_w \end{bmatrix} \end{aligned}$$

System model

The models explained in the previous two paragraphs have to be coupled to become the system model that is used for filter design. Figure 5 shows the detailed plant and the Kalman-Bucy filter structure. The linear aircraft model (eq. (4)) can be combined with Dryden's

turbulence model (eq. (9)) and therefore the disturbance input $\mathbf{r}(t)$ to the model via \mathbf{B}_{Dry} is white noise and the

KF derivation constraints are fulfilled. Because of the immeasurability of $\mathbf{r}(t)$ the input vector is $\mathbf{u} = \begin{bmatrix} 0 & u_{a/c} \end{bmatrix}^T$. For the estimation of a bias in the AOA measurement an additional state (α_{bias}) has to be modelled as a random walk process. The system model state space equations

$$\begin{aligned} \tilde{\mathbf{x}} &= \mathbf{A} \tilde{\mathbf{x}} + \mathbf{B} \mathbf{u} \\ \tilde{\mathbf{y}} &= \mathbf{C} \tilde{\mathbf{x}} \\ \tilde{\mathbf{y}}^* &= \mathbf{C}^* \tilde{\mathbf{x}} \end{aligned} \quad (10)$$

can be written explicitly as follows:

$$\begin{aligned} \begin{bmatrix} \tilde{\mathbf{x}} \\ \tilde{\mathbf{y}} \end{bmatrix} &= \begin{bmatrix} \tilde{\mathbf{x}}_{\text{Dry}} \\ \tilde{\mathbf{x}}_{a/c} \\ \alpha_{\text{bias}} \end{bmatrix} = \begin{bmatrix} \mathbf{A}_{\text{Dry}} & 0 & 0 \\ \mathbf{E}_{a/c=\text{Dry}} & \mathbf{A}_{a/c} & 0 \\ 0 & 0 & 0 \end{bmatrix} \begin{bmatrix} \tilde{\mathbf{x}}_{\text{Dry}} \\ \tilde{\mathbf{x}}_{a/c} \\ \alpha_{\text{bias}} \end{bmatrix} + \dots \\ &\dots + \begin{bmatrix} \mathbf{B}_{\text{Dry}} & 0 \\ 0 & \mathbf{B}_{a/c} \\ 0 & 0 \end{bmatrix} \begin{bmatrix} 0 \\ u_{a/c} \end{bmatrix} \\ \begin{bmatrix} \tilde{\mathbf{y}} \end{bmatrix} &= \begin{bmatrix} \tilde{q}_k \\ \tilde{\alpha} \\ \tilde{V}_A \\ \tilde{\Theta} \\ \tilde{H} \end{bmatrix} = \begin{bmatrix} \mathbf{F}_{a/c=\text{Dry}} & \mathbf{C}_{a/c} & \mathbf{C}_{\text{bias}} \end{bmatrix} \begin{bmatrix} \tilde{\mathbf{x}}_{\text{Dry}} \\ \tilde{\mathbf{x}}_{a/c} \\ \alpha_{\text{bias}} \end{bmatrix} \\ \mathbf{C}_{\text{bias}} &= \begin{bmatrix} 0 & 1 & 0 & 0 & 0 \end{bmatrix}^T \\ \begin{bmatrix} \tilde{\mathbf{y}}^* \end{bmatrix} &= \begin{bmatrix} \tilde{y} \\ \tilde{\alpha}_k \\ \tilde{\alpha}_w \\ \tilde{\alpha}_{\text{bias}} \\ \tilde{V}_w \end{bmatrix} = \begin{bmatrix} 0 & 0 & 0 & 0 & \mathbf{C}_{\text{bias}} \\ 0 & 1 & 0 & 0 & 0 \\ 0 & 0 & 0 & 0 & 0 \\ 0 & 0 & 0 & 0 & 1 \\ 0 & 0 & 1 & 0 & 0 \end{bmatrix} \begin{bmatrix} \tilde{\mathbf{x}}_{\text{Dry}} \\ \tilde{\mathbf{x}}_{a/c} \\ \alpha_{\text{bias}} \end{bmatrix} \end{aligned} \quad (11)$$

Observability

A system is observable if eq. (12) is true.

$$\text{rank} \begin{pmatrix} \lambda_i \mathbf{I} - \mathbf{A} \\ -\mathbf{C} \end{pmatrix} = n \quad (12)$$

Where λ_i are the Eigen values and n is the number of states [12]. The system is observable because of the coupling in the system matrix \mathbf{A} caused by

$\mathbf{E}_{a/c=\text{Dry}} \mathbf{C}$ and in the measurement matrix \mathbf{C} caused by $\mathbf{F}_{a/c=\text{Dry}} \mathbf{C}$, so this requirement is fulfilled.

3 KALMAN-BUCY FILTER DESIGN

Measurement noise characteristics

The covariance matrix $\underline{\Theta}$, describing the measurement noise, is determined by datasheet³ [13] and the wind tunnel measurements explained in [6]. The altitudes standard deviation σ_H is an approximation.

$$\underline{\Theta} = \text{diag} \begin{bmatrix} \sigma_{q_k}^2 \\ \sigma_{\alpha}^2 \\ \sigma_{V_A}^2 \\ \sigma_{\Theta}^2 \\ \sigma_H^2 \end{bmatrix} = \text{diag} \begin{bmatrix} \sigma_{q_k}^2 \\ \sigma_{\alpha}^2 \\ \sigma_{V_A}^2 \\ \sigma_{\Theta}^2 \\ \sigma_H^2 \end{bmatrix} = \text{diag} \begin{bmatrix} (0.6\pi/180)^2 \\ (0.5\pi/180)^2 \\ (0.35)^2 \\ (0.2\pi/180)^2 \\ 1 \end{bmatrix}$$

Process noise characteristics

For this particular filter design model uncertainties are modeled via process noise (ξ_2 and ξ_1). The first three system states of \tilde{x} are the turbulence states and the model uncertainties are described via ξ_2 . The design takes the white noise source r of the Dryden's turbulence model into account. The chosen standard deviation for process noise describing model uncertainties are in the same value range as for comparable measurement noise standard deviation.

$$\underline{\Xi} = \text{diag} \begin{bmatrix} \xi_2^2 \\ \xi_2^2 \\ \xi_2^2 \\ \xi_1^2 \end{bmatrix} + \text{diag} \begin{bmatrix} 0 \\ 1 \\ 1 \\ 0 \\ 0 \\ 0 \\ 0 \\ 0 \\ 0 \end{bmatrix} = \text{diag} \begin{bmatrix} \xi_{\alpha_W}^2 \\ \xi_{\alpha_W}^2 + 1 \\ \xi_{V_W}^2 + 1 \\ \xi_{q_k}^2 \\ \xi_{\alpha_K}^2 \\ \xi_{V_K}^2 \\ \xi_{\Theta}^2 \\ \xi_H^2 \\ \xi_{\alpha_{bias}}^2 \end{bmatrix}$$

$$\underline{\Xi} = \text{diag} \begin{bmatrix} (0.1\pi/180)^2 \\ (0.5\pi/180)^2 + 1 \\ (0.35)^2 + 1 \\ (0.6\pi/180)^2 \\ (0.5\pi/180)^2 \\ (0.35)^2 \\ (0.2\pi/180)^2 \\ 1^2 \\ (0.35)^2 \end{bmatrix}$$

³ σ_{pk} is calculated from angular random walk and σ_{Θ} is set equal to repeatability

The resulting Kalman gain matrix \underline{H} and the estimation error covariance matrix $\underline{\Sigma}$ are in the appendix.

4 RESULTS

The simulations were performed on a standard PC. The system model and the Kalman-Bucy filter were implemented in SIMULINK, as shown in Fig. 5. A 4th order Runge-Kutta algorithm was chosen for numerical integration with a step size of 0.02 s.

Case 1: nominal condition

Figure 6 to 10 show simulation results for the derived system model and the Kalman-Bucy filter. The aircraft is in trimmed condition, disturbed by Dryden turbulence and responding to elevator block inputs, see Fig. 6. Measured states have the index "meas" and the estimated states are marked with \sim . The strength of measurement and process noise is as defined in section 3. After 12 seconds a bias of $\alpha_{bias}=1^\circ$ is introduced as can be seen in Fig. 7 and at the spike in Fig. 8. In Figure 7 the immeasurable turbulence states and the bias state are compared with their estimates. Figure 8 shows time histories of the error ($\Delta = x - \tilde{x}$) between the state variables and their estimates and probability distributions of the error. In these plots the blue line indicates the mean value and the red lines indicate the standard deviations of the error. The correlation between the aircraft states, the immeasurable turbulence states and their estimates is good. The mean errors and the standard deviations are small. The bias in the α measurement is well estimated. Figure 9 and 10 show the Fourier analysed signals, in a logarithmic representation, of α_W and the estimated $\tilde{\alpha}_W$ as well as V_W and the estimates \tilde{V}_W . Up to 2 Hz, which correspond to the short period mode of the aircraft, α_W and $\tilde{\alpha}_W$ are close to each other. For higher frequencies, which are not of interest, the estimation is too high. The correlation of V_W and its estimation is good up to 1 Hz. For higher frequencies \tilde{V}_W is underestimated.

Case 2 (discrete gust condition)

To analyse the influence of model uncertainties, disturbance inputs of the turbulence model to the aircraft model are replaced by discrete ramp gust for α_W (after 2 sec) and V_W (after 17 sec). The results are shown in Fig. 11 and Fig. 12. The Kalman-Bucy filter and the disturbances by process and measurement noise for the aircraft are the same as for the nominal case. Figure 11 and 12 show the robustness of the filter approach. Even for a different disturbance type (discrete ramp gusts) the estimates for wind induced disturbances are good. The analysed errors show that the precision of the estimation equals the nominal case. The mean error and the standard deviations are small. Due to the measurement noise and the small stimulated frequency range by the discrete gust the Fourier analysed signals (Fig. 13 - 14) show an unsufficient correlation for frequencies above 0.2 Hz.

5 CONCLUSION

The application of Kalman-Bucy filtering with a combination of a linear aircraft model and Dryden's turbulence model to improve the measurement of the aircraft states and to estimate the immeasurable wind states has proved to be feasible. Simulation results show a good and broadband correlation between the states and their estimates up to 2 Hz (short period mode). The estimations are robust against variations of the disturbance model and a bias in the AOA measurement.

For operational use in an aircraft this approach shall be developed further using an extended Kalman Filter based on the described concept and a non-linear aircraft model. The EKF has to be carefully tuned by observation and minimizing of the estimation error covariance matrix. The observability of each state under different conditions, e.g. no turbulence, has to be analysed.

APPENDIX

For the reference state ($V=20$ m/s; $H=100$ m; $\gamma=0^\circ$) and numerical derivation the aircraft model of the UAV ALEXIS [4], [6] is given by:

$$\begin{bmatrix} \dot{q}_K \\ \dot{\alpha}_K \\ \dot{V}_K \\ \dot{\Theta} \\ \dot{H} \end{bmatrix} = \begin{bmatrix} -10.5 & -50 & 0 & 0 & 0 \\ 0.9 & -11 & -0.049 & 0 & 0 \\ -0.36 & 10.37 & -0.092 & -9.81 & 0 \\ 1 & 0 & 0 & 0 & 0 \\ 0 & -20 & 0 & 20 & 0 \end{bmatrix} \begin{bmatrix} q_K \\ \alpha_K \\ V_K \\ \Theta \\ H \end{bmatrix} + \begin{bmatrix} -134 & 0 \\ -1 & 0 \\ -0.09 & 0.004 \\ 0 & 0 \\ 0 & 0 \end{bmatrix} \begin{bmatrix} \eta \\ \eta_F \end{bmatrix} + \begin{bmatrix} 50 & 0 \\ 11 & 0.049 \\ 10.36 & 0.092 \\ 0 & 0 \\ 0 & 0 \end{bmatrix} \begin{bmatrix} \alpha_W \\ V_W \end{bmatrix} + \begin{bmatrix} \xi_{q_K} \\ \xi_{\alpha_K} \\ \xi_{V_K} \\ \xi_{\Theta} \\ \xi_H \end{bmatrix}$$

$$\begin{bmatrix} q_K \\ \alpha \\ V_A \\ \Theta \\ H \end{bmatrix} = \begin{bmatrix} 1 & 0 & 0 & 0 & 0 \\ 0 & 1 & 0 & 0 & 0 \\ 0 & 0 & 1 & 0 & 0 \\ 0 & 0 & 0 & 1 & 0 \\ 0 & 0 & 0 & 0 & 1 \end{bmatrix} \begin{bmatrix} q_K \\ \alpha_K \\ V_K \\ \Theta \\ H \end{bmatrix} + \begin{bmatrix} 0 & 0 \\ -1 & 0 \\ 0 & -1 \\ 0 & 0 \\ 0 & 0 \end{bmatrix} \begin{bmatrix} \alpha_W \\ V_W \end{bmatrix} + \begin{bmatrix} \theta_{q_K} \\ \theta_{\alpha} \\ \theta_{V_A} \\ \theta_{\Theta} \\ \theta_H \end{bmatrix}$$

The resulting Kalman gain Matrix $\underline{\underline{H}}$ and the estimation error covariance matrix $\underline{\underline{\Sigma}}$ are:

$$\underline{\underline{H}} = \begin{bmatrix} 0.034 & -0.22 & 0.0005 & -0.1383 & 0.0029 \\ 35.43 & -105.67 & -0.0507 & 12.41 & -0.0186 \\ -1.16 & 2.2 & -3.05 & -9.26 & -0.0468 \\ 33.8 & -30.9 & -0.0069 & 7.88 & -0.0004 \\ 10.22 & -6.68 & -0.0473 & 11.06 & -0.0186 \\ -8.9 & 6.37 & 0.078 & -17.85 & -0.0242 \\ 0.8759 & 0.006 & -0.0009 & 2.97 & -0.0005 \\ -3.811 & -1.41 & 0.1841 & -38.44 & 1.3 \\ 3.75 & 1.86 & -0.0009 & 1.385 & -0.0001 \end{bmatrix}$$

$$\underline{\underline{\Sigma}} = \begin{bmatrix} 0.024 & -0.0001 & 0.0003 & 0.00 & -0.0002 & 0.0004 & -0.00 & 0.003 & 0.00 \\ -0.0001 & 0.0109 & 0.0064 & 0.0039 & 0.0024 & -0.0002 & 0.0002 & -0.0186 & 0.0004 \\ 0.0003 & 0.0064 & 0.6793 & -0.0001 & 0.0066 & 0.3058 & -0.0001 & -0.046 & -0.00 \\ 0.00 & 0.0039 & -0.0001 & 0.0037 & 0.0011 & -0.001 & -0.0001 & -0.0004 & 0.0004 \\ -0.0002 & 0.0024 & 0.0066 & 0.0011 & 0.0018 & -0.0008 & 0.0001 & -0.0186 & 0.0001 \\ 0.0004 & 0.0002 & 0.3058 & -0.001 & -0.0008 & 0.3154 & -0.0002 & -0.024 & -0.0001 \\ -0.00 & 0.0002 & -0.0001 & 0.0001 & 0.0001 & -0.002 & 0.000 & -0.0005 & 0.00 \\ 0.003 & -0.0186 & -0.0468 & -0.0004 & -0.0186 & -0.024 & -0.005 & 1.3 & -0.0001 \\ 0.00 & 0.0004 & -0.00 & 0.0004 & 0.0001 & -0.0001 & 0.00 & -0.0001 & 0.0004 \end{bmatrix}$$

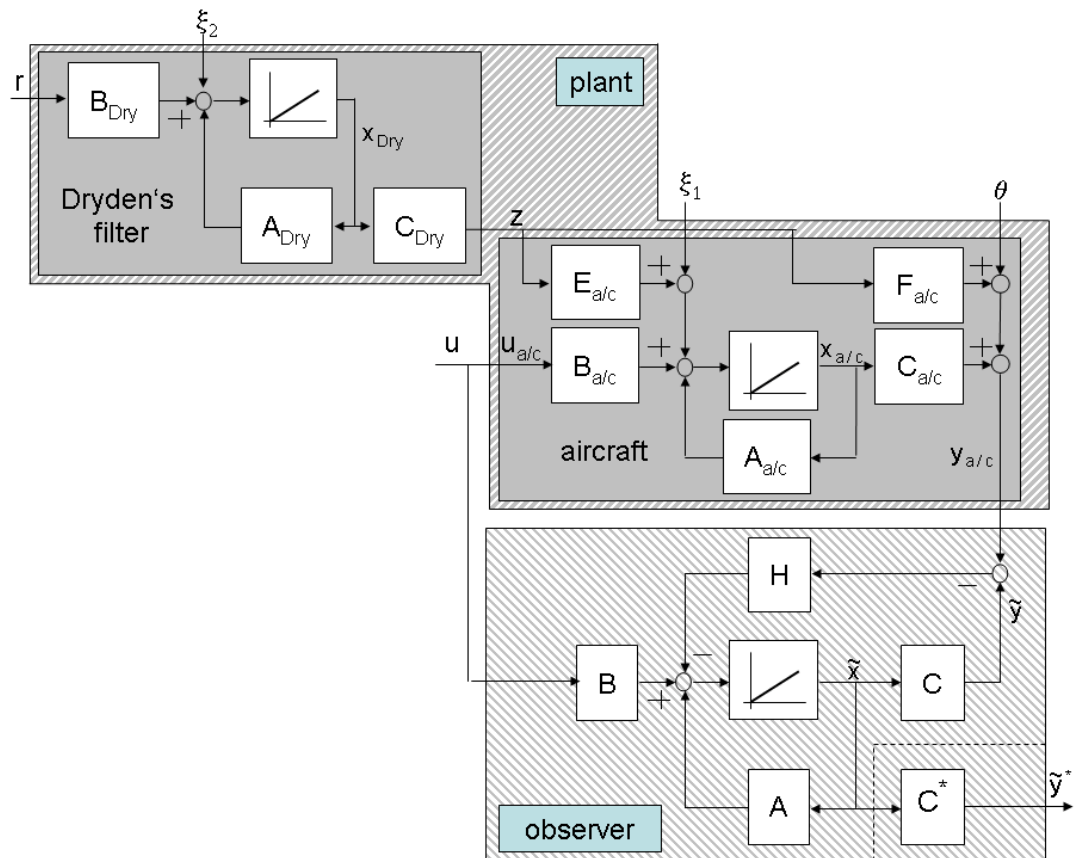


Fig. 5: Detailed plant and Kalman-Bucy filter structure

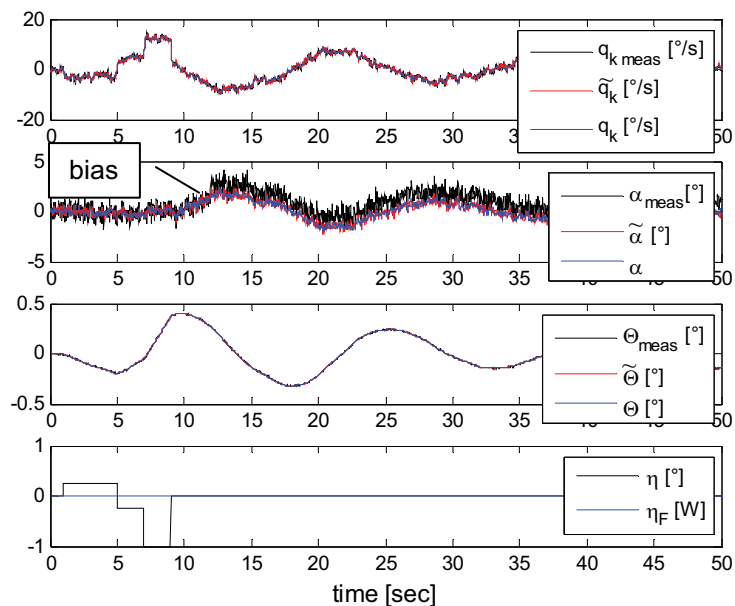


Fig. 6: Simulated time histories of aircraft states, their measurements and the Kalman-Bucy filter estimates (case 1)

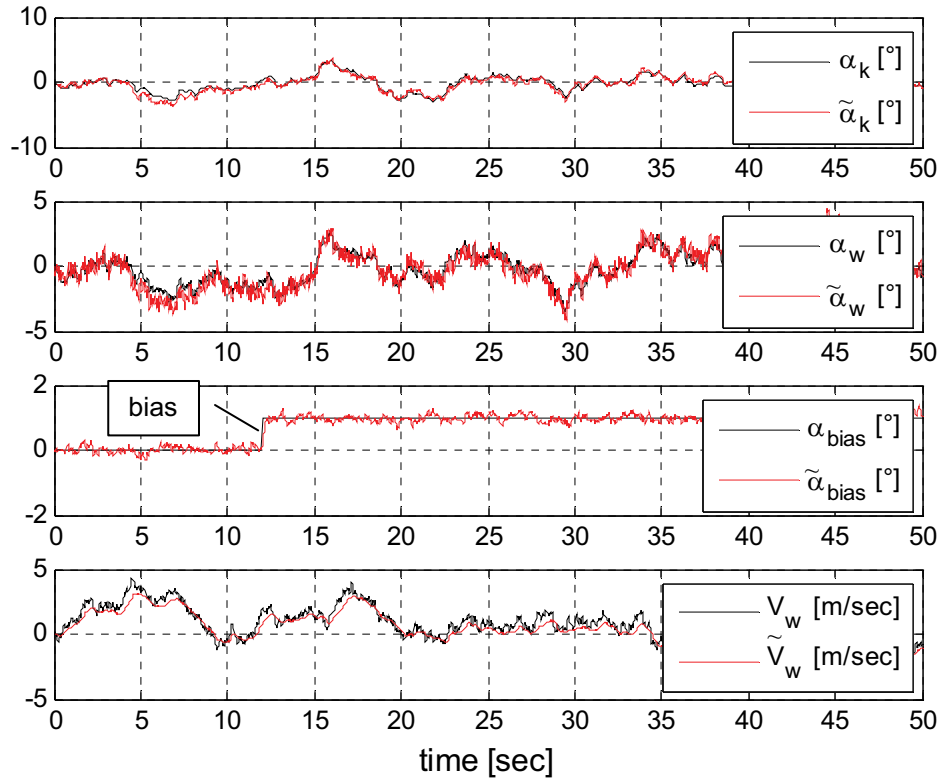


Fig. 7: Simulated time histories of immeasurable states and Kalman-Bucy filter estimates (case 1)

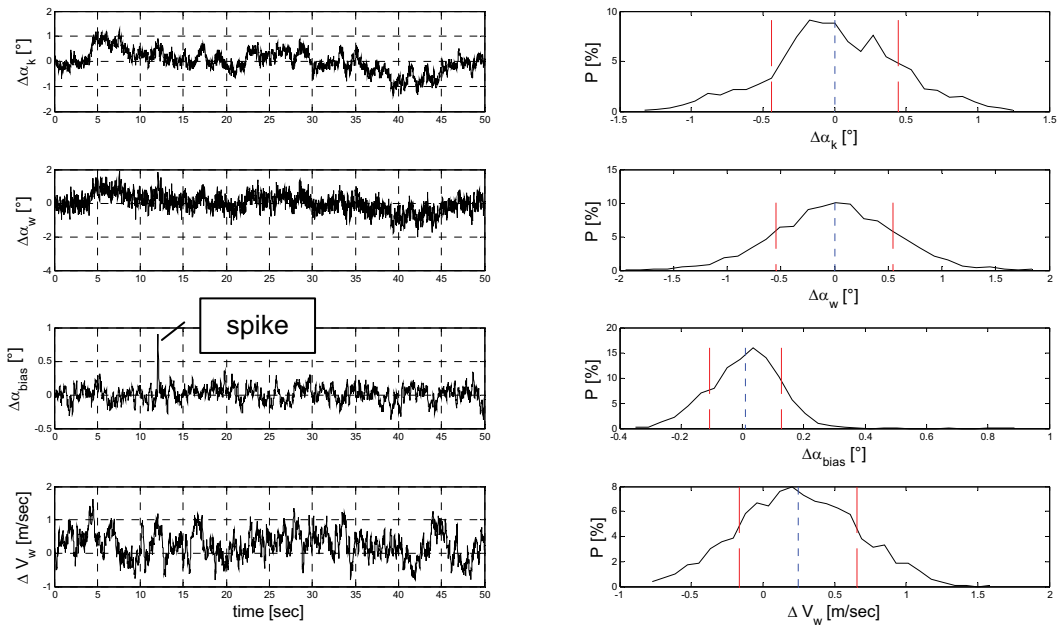


Fig. 8: Error analysis of the immeasurable states and the Kalman-Bucy filter estimates (case1)

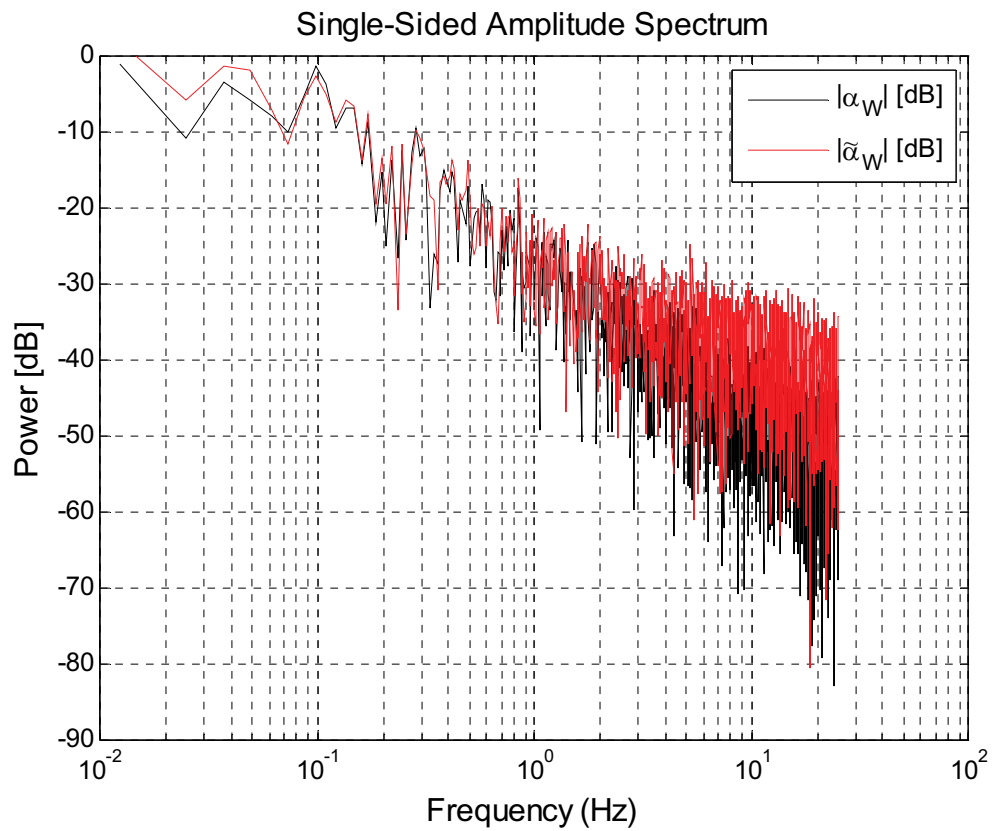


Fig. 9: Fourier analysis of α_W and its estimation (case1)

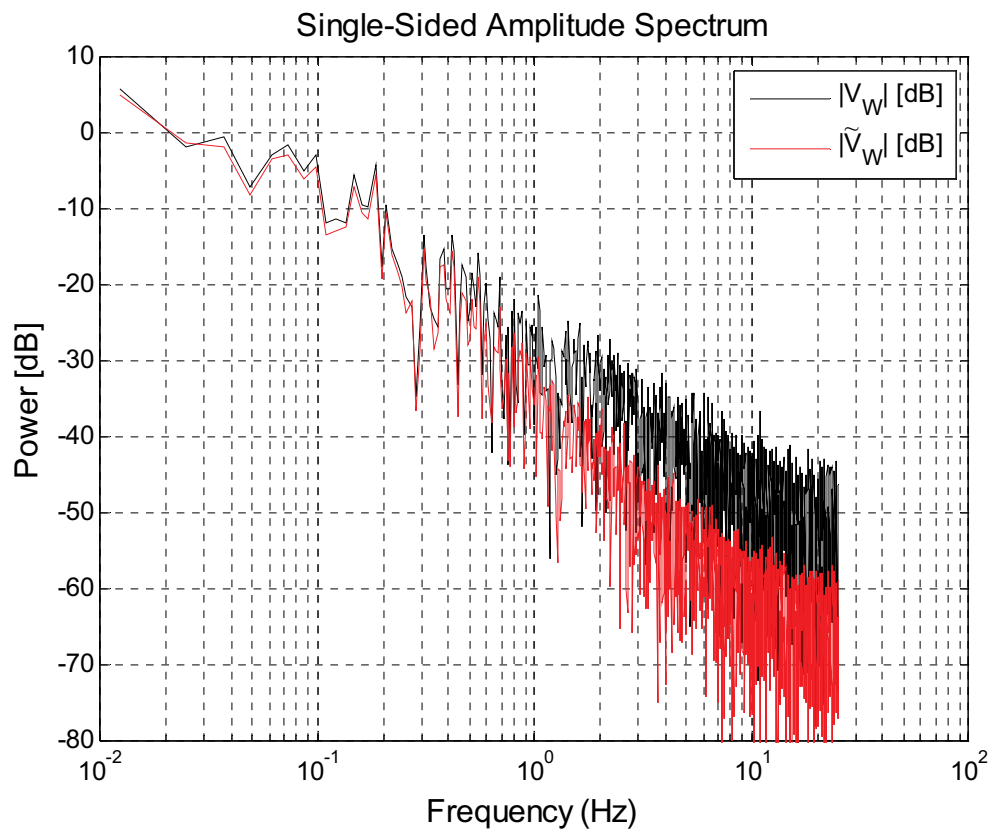


Fig. 10: Fourier analysis of V_W and its estimation (case1)

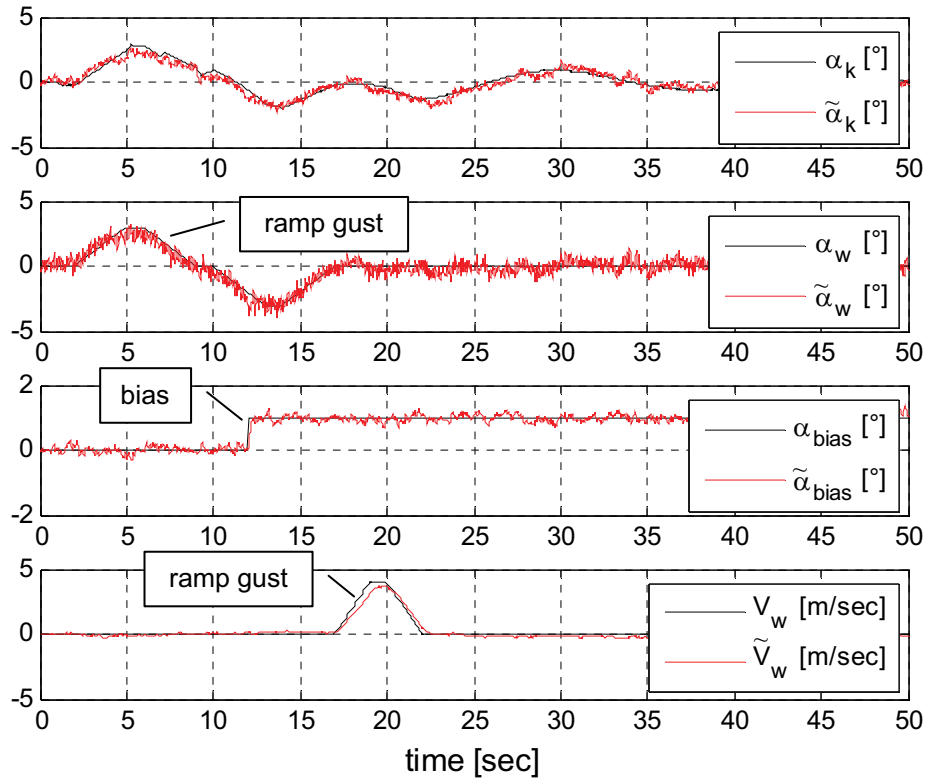


Fig. 11: Simulated time histories of immeasurable states and Kalman-Bucy filter estimates (case 2)

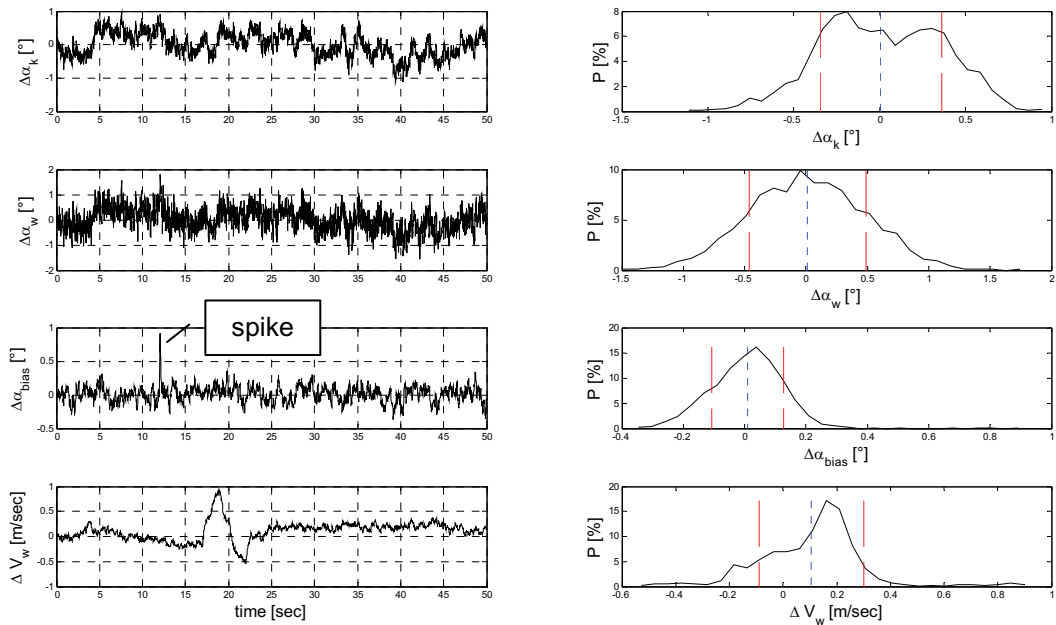


Fig. 12: Error analysis of the immeasurable states and the Kalman-Bucy filter estimates (case 2)

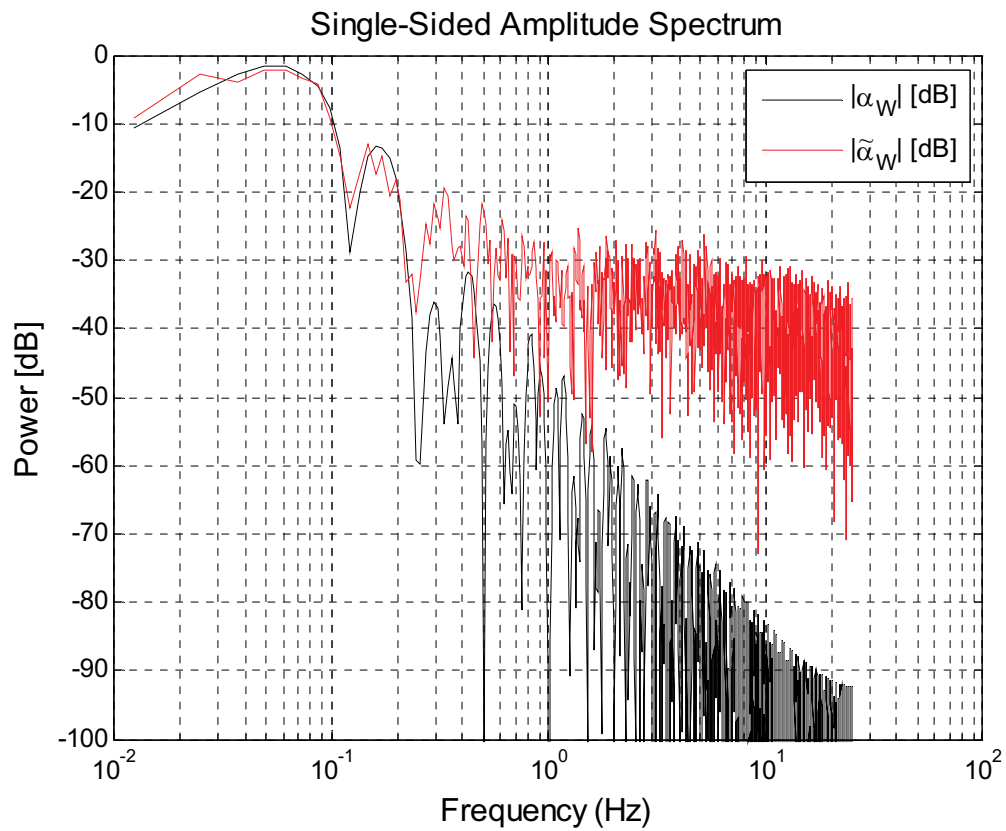


Fig. 13: Fourier analysis of α_W and its estimation (case 2)

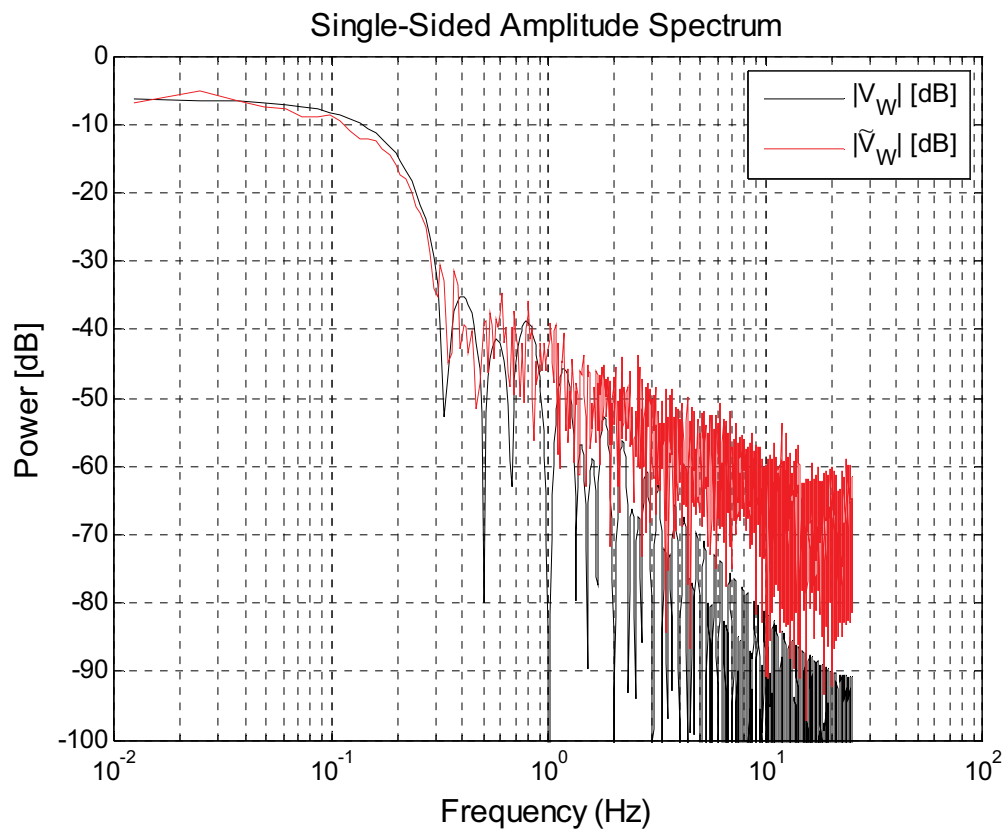


Fig. 14: Fourier analysis of V_W and its estimation (case 2)

References

- [1] K. Wise: "Flight testing of the X-45A J-UCAS Computational Alpha-Beta System", AIAA Guidance, Navigation and Control Conference and Exhibit, Keystone Colorado, 21-24 August 2006
- [2] M. Heller, S. Myschik, F. Holzapfel, G. Sachs: "Low-cost approach based on navigation data for determining angles of attack and sideslip for small aircraft", AIAA Guidance, Navigation and Control Conference and Exhibit, Austin, Texas, 11-14 August 2003
- [3] S. Myschik, M. Heller, F. Holzapfel, G. Sachs: "Low-cost System zur Bestimmung von Anstell- und Schiebewinkel für Kleinflugzeuge", Deutscher Luft und Raumfahrt Kongress 2003, München
- [4] A. Hoffmann, F. Schindler, R. Luckner: "Luftdatensystem für das UAV ALEXIS", Deutscher Luft und Raumfahrt Kongress, Darmstadt, 2008
- [5] C. Braga de Mendonca: "Adaptive stochastic Filtering for online aircraft flight path reconstruction", Journal of aircraft, Vol. 44, No.5, September-October 2007
- [6] A. Hoffmann, R. Luckner: "Precise and broadband angle of attack determination in presence of atmospheric turbulence and measurement noise", CEAS, Manchester, 2009
- [7] K.-U. Hahn: „Verfahren zur Reduzierung der Turbulenz- und Böeneinflüsse auf das Flugverhalten von Luftfahrzeugen und Steuereinrichtungen hierfür“. Bundesrepublik Deutschland, Patent Nr. 102005020660, München Germany, 2007
- [8] A. Hoffmann, F. Schindler, R. Luckner: "IFSys a TU Berlin student project", CEAS, Berlin, 2007
- [9] F. Schindler: "Entwicklung, Konstruktion und Kalibrierung eines Luftdatensystems, mit Verbesserung der Signalqualität durch komplementäre Filterung, für ein UAV", Diplomarbeit, Fachgebiet Flugmechanik, Flugregelung und Aeroelastizität, Berlin, 2008
- [10] K. Müller: "Entwurf robuster Regelungen", ISBN 3-519-06173-2, Teubner, Stuttgart, 1996
- [11] R. Brockhaus: „Flugregelung“, ISBN 3-540-55416-5, Springer, 2. bearb. Auflage, 2001
- [12] R. King: „Regelungstechnik II“, Skript, TU Berlin, Fachgebiet Mess- und Regelungstechnik, Institut für Prozess- und Anlagentechnik, WS06/07
- [13] Microstrain: "Detailed Specification for 3DM-GX1", www.microstrain.com, July 2009